JOURNAL OF CATALYSIS 122, 178–192 (1990)

Photocatalytic Degradation of Organic Water Contaminants: Mechanisms Involving Hydroxyl Radical Attack

CRAIG S. TURCHI AND DAVID F. OLLIS

Department of Chemical Engineering, North Carolina State University, Raleigh, North Carolina 27695-7905

Received August 18, 1989; revised October 11, 1989

Hydroxyl and other oxygen-containing radicals are known to be present during the degradation of organic water pollutants in illuminated TiO_2 photocatalyst slurries. It is proposed that the hydroxyl radical, OH·, is the primary oxidant in the photocatalytic system. Four possible mechanisms are suggested, all based on OH· attack of the organic reactant. The cases of reaction on the surface, in the fluid, and via a Rideal mechanism are shown to yield expressions similar to Langmuir–Hinshelwood (L–H) rate forms. Compared with traditional L–H constants, the derived kinetic parameters represent fundamentally different reactions and properties. A rate parameter independent of organic reactant is predicted by the model and substantiated by experimental degradation data. On the basis of these model results, the kinetic parameters for the photocatalytic degradation may be estimated from data on the photocatalyst's physical properties, the knowledge of electron-hole recombination and trapping rates, and the values of second-order reaction rate constants for hydroxyl radicals. © 1990 Academic Press, Inc.

INTRODUCTION

The investigation of any chemical reaction has often followed a three-step sequence: determination of reaction stoichiometry, description of the observed kinetics, and finally, development of plausible mechanisms. Thus far, these first two steps have accounted for most research in heterogeneous photocatalysis. For example, in studies of aqueous chlorocarbon degradations, mass balances on chloride and carbon, as well as oxygen uptake studies, have indicated the reaction stoichiometry. In addition, the use of Langmuir–Hinshelwood (L–H) rate equations has provided reasonable simulations of the observed degradation kinetics. It now remains to postulate reaction mechanisms which are consistent with the observed stoichiometry and kinetics, and which are plausible considering the known physical and electronic properties of the illuminated semiconductor–water system. In turn, the proposed mechanisms will suggest further studies and calculations which may support or refute the likelihood of a given mechanism and thereby promote an increased understanding of the photocatalytic reaction.

The effectiveness of heterogeneous photocatalysis for the total oxidation of organic and halo-organic water contaminants has been verified by numerous researchers (*1–6*). Additional work has examined the effect of dissolved oxygen concentration (*7, 8*), light intensity (*9–11*), photocatalyst particle size (*12, 13*), and the practicality of immobilizing the photocatalyst (*14–16*). An interesting aspect of the accumulating kinetic data is that in a given reactor the observed disappearance rates for a variety of different chemical compounds are remarkably similar (*1, 5*). This behavior might be expected for a reaction involving a highly energetic species (e.g., photo-excited electron or hole). Yet, since surface adsorption is required for interaction with these species, differences in the affinity for adsorption of different chemical compounds should give rise to a broad range of observed reaction rates. If, on the other hand, a surface species such as hydroxyl radicals acted as a reactive intermediate between the photo-excited semiconductor and oxidizable or-

0021-9517/90 $3.00

ganics, the similarity of reaction rates could be explained by a rate-limiting step consisting of hydroxyl radical formation or by the relatively uniform rate with which hydroxyl radicals attack many organics (*17*).

In this paper, we outline evidence implicating the hydroxyl radical, OH·, as the primary oxidant in the photocatalytic oxidation of organics. A single semiconductor particle is modeled to determine the photocatalytic reaction rate per particle. The modeling of a single particle will allow the results to be incorporated into an appropriate radiation intensity profile to solve for an overall degradation rate in a typical illuminated slurry reactor. The derived kinetic model is based on hydroxyl radical attack of the organic reactant. Four cases are investigated:

(I) Reaction occurs while both species are adsorbed.

(II) A nonbound radical reacts with an adsorbed organic molecule.

(III) An adsorbed radical reacts with a free organic molecule arriving at the catalyst surface.

(IV) Reaction occurs between two free species in the fluid phase.

Similar rate forms are found for each case. The four kinetic models developed are all consistent with reported initial rate and temporal degradation data and are no more complicated than empirical expressions frequently used to describe photocatalytic degradations.

EVIDENCE FOR OH· AS THE PRIMARY OXIDANT

It is well documented that the surface of TiO_2 is readily hydroxylated when the semiconductor is in contact with moisture (*18, 19*). Both dissociated and molecular water are bound to the surface. When H_2O dissociates on a pure TiO_2 surface, two distinctive hydroxyl groups are formed (*20, 21*) (Fig. 1). Boehm (*20*) has estimated that the theoretical maximum surface coverage is 5–15 OH^-/nm^2, depending on which crystal plane is being considered. Infrared evidence and spatial considerations suggest that certain crystal faces, (100) and (101), bond only molecular H_2O, while others, (110) and (001), produce hydroxyl group pairs as in Fig. 1 (*21–23*). Assuming that anatase particles consist of a mixture of these surface planes (*23*), complete surface coverage by OH^- and H_2O should be represented by a surface density of 5–15 OH^-/nm^2, depending on the crystal faces present (that is, on production and pretreatment techniques). Most researchers report surface coverages of 7–10 OH^-/nm^2 on room

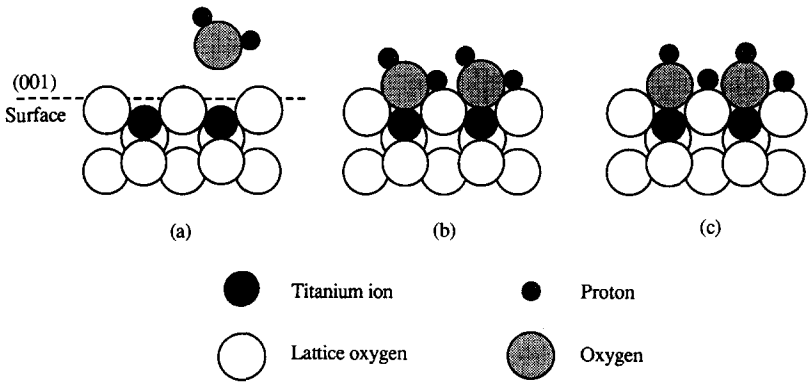

FIG. 1. Surface hydroxyl groups on TiO_2 (*20*). (a) Hydroxyl-free surface; (b) physical adsorption of water; (c) dissociation of water, giving rise to two distinct OH^- groups.

TABLE 1

Photocatalytic Reaction Scheme

Excitation			
	TiO_2	$\xrightarrow{h\nu} e^- + h^+$	(T1)
Adsorption			
	$O_L^{2-} + Ti^{IV} + H_2O$	$\rightleftharpoons O_LH^- + Ti^{IV}\text{–}OH^-$	(T2-a)[a]
	$Ti^{IV} + H_2O$	$\rightleftharpoons Ti^{IV}\text{–}H_2O$	(T2-b)
	site $+ R_1$	$\rightleftharpoons R_{1,ads}$	(T3)
	$OH\cdot + Ti^{IV}$	$\rightleftharpoons Ti^{IV}\rangle OH\cdot$	(T4)
Recombination			
	$e^- + h^+$	$\rightarrow$ heat	(T5)
Trapping			
	$Ti^{IV}\text{–}OH^- + h^+$	$\rightleftharpoons Ti^{IV}\rangle OH\cdot$	(T6-a)
	$Ti^{IV}\text{–}H_2O + h^+$	$\rightleftharpoons Ti^{IV}\rangle OH\cdot + H^+$	(T6-b)
	$R_{i,ads} + h^+$	$\rightleftharpoons R_{i,ads}^+$	(T7)
	$Ti^{IV} + e^-$	$\rightleftharpoons Ti^{III}$	(T8-a)
	$Ti^{III} + O_2$	$\rightleftharpoons Ti^{IV}\text{–}O_2^-$	(T8-b)
Hydroxyl Attack			
Case I	$Ti^{IV}\rangle OH\cdot + R_{1,ads}$	$\rightarrow Ti^{IV} + R_{2,ads}$	(T9)
Case II	$OH\cdot + R_{1,ads}$	$\rightarrow R_{2,ads}$	(T10)
Case III	$Ti^{IV}\rangle OH\cdot + R_1$	$\rightarrow Ti^{IV} + R_2$	(T11)
Case IV	$OH\cdot + R_1$	$\rightarrow R_2$	(T12)
Reactions of other radicals			
	$e^- + Ti^{IV}\text{–}O_2^- + 2(H^+)$	$\rightleftharpoons Ti^{IV}(H_2O_2)$	(T13)
	$Ti^{IV}\text{–}O_2^- + (H^+)$	$\rightleftharpoons Ti^{IV}(HO_2)$	(T14)
	$(H_2O_2) + (OH\cdot)$	$\rightleftharpoons (HO_2^-) + (H_2O)$	(T15)

Note. Species in parentheses may be adsorbed or in the aqueous phase.

[a] Involves one lattice oxygen; see Fig. 1, text.

temperature TiO_2 (*22, 24–27*). These results are consistent with a particle completely covered by bound OH^- and H_2O.

A complete sequence of elementary steps representing the proposed mechanisms is summarized in Table 1 (Eqs. (T1)–(T15)). The four cases cited earlier are given as reactions (T9) through (T12). Under near-UV illumination, electron-hole pairs are formed in the semiconductor (reaction (T1)). These two species may recombine in the bulk lattice or migrate to the surface where they can react with adsorbates. Since OH^- and H_2O groups are the most abundant adsorbates, it seems likely that holes will react with these species. For oxidation of OH^- or H_2O to occur, the oxidation potential for reactions (T6-a) and (T6-b) must lie above (i.e., be more negative than) the position of the semiconductor valence band, E_v. The semiconductor band potentials are functions of pH, with the valence band of anatase lying at roughly +2.6 V (vs NHE) at neutral pH and varying as −0.059 V/pH unit (*28–30*). The oxidation potentials for the reactions of Eq. (T6) remain above E_v (thermodynamically favorable) throughout the entire pH range, with reaction (T6-a) favored at high pH and (T6-b) favored at low pH (*31*). Thus, under both acidic and basic conditions, the oxidation of surface-bound OH^- and H_2O by TiO_2 valence band holes to form $OH\cdot$ is thermodynamically possible and expected.

The oxidation potentials for many organic compounds are also above the E_v of anatase, so, at least thermodynamically, they should be able to interact directly with holes at the photocatalyst surface. However, experiments run in water-free, aer-

TABLE 2

Kinetic Isotope Effect on Initial Photodegradation Rate (*35*)

System	Relative rate
$TiO_2/O_2/(CH_3)_2CHOH/H_2O$	1.0
$TiO_2/O_2/(CD_3)_2CDOD/H_2O$	1.0
$TiO_2/O_2/(CD_3)_2CDOD/D_2O$	0.36

ated organic solvents have displayed only partial oxidation of organics. The complete mineralization to CO_2, common in aqueous solutions, was not witnessed (*32–34*). The presence of water or hydroxyl groups appears to be essential for complete oxidative destruction of organic reactants.

Cunningham and Srijaranai (*35*) have demonstrated a H_2O/D_2O kinetic isotope effect in the photocatalyzed oxidation of isopropanol in TiO_2 and ZnO slurries. Their findings are summarized in Table 2. Substitution of deuterium for hydrogen on the organic reactant had no effect on the observed initial reaction rate. Apparently, direct reaction between the organic and the photocatalyst valence band holes is not significant. In contrast, replacing the H_2O solvent with D_2O led to a decrease in rate. These results imply that the rate-limiting reaction step is the formation of active oxygen species (OH· or OD·) through reactions involving the solvent. The observed decrease in rate for the D_2O solvent arises from the higher energy requirement for the formation of the radical because the O–D bond has a lower ground energy level than the O–H bond. The photo-generated radical species subsequently attack and degrade the organic reactant.

Intermediates detected during the photocatalytic degradation of aromatic compounds are typically hydroxylated structures (*8, 36–40*). These intermediates are consistent with those found when similar aromatics are reacted with a known source of hydroxyl radicals (*28, 41–43*), further suggesting that OH· is the primary attacking species.

Lastly, ESR studies have verified the existence of OH· in aqueous solutions of illuminated TiO_2 (*44, 45*). While the radical–spin trap complex is detected in the liquid phase, it is not possible to distinguish whether the actual trapping reaction occurs on the semiconductor surface or in solution. Studies of a gas–solid system using hydroxylated TiO_2 have also detected the presence of OH· (*49*). The perhydroxyl radical $HO_2^{\cdot}$ has also been detected (*45, 46*). Likely routes for $HO_2^{\cdot}$ formation include the protonation of superoxide (reaction (T14)) and the reaction of OH· with photo-generated hydrogen peroxide (reaction (T15)), as H_2O_2 is known to be present (*8, 47, 48, 50*).

In summary, the experimental evidence supporting the concept of OH· as the primary oxidizing species includes:

- ESR detection of OH· as the most abundant radical species.
- Necessity of photocatalyst surface hydroxylation for organic degradation.
- Kinetic isotope effect demonstrating the kinetic importance of the OH· formation step.
- Formation of highly hydroxylated reaction intermediates.

While OH· is clearly produced by reaction at the photocatalyst surface, it may desorb and react in the fluid phase (*44, 46, 51, 52*). Hence, several possibilities exist for reaction pathways between the radical species and the organic molecules depending on which, if any, of the reacting molecules are adsorbed to the photocatalyst surface at the moment of reaction.

REACTION MECHANISM

A sequence of elementary steps which describe the initial photocatalytic oxidation mechanism is presented in Table 1. The purpose of this scheme is to reasonably depict the degradation process while maintaining enough simplicity to be useful for the development of kinetic equations. Certain reactions, which are separated into two steps or include two similar events (e.g.,

(T6)), are represented by one overall reaction rate.

The initiating step in photocatalysis is the excitation of the semiconductor by radiation sufficiently energetic ($\lambda < 380$ nm for anatase) to produce electron-hole pairs (reaction (T1)). The typically low quantum yield of photocatalytic reactions is due to the high rate of recombination (reaction (T5)). Recombination can be avoided if these mobile species are separated and subsequently "trapped" by surface adsorbates or other sites. In sufficiently large semiconductor particles this separation is aided by the formation of a potential gradient or *space-charge* region near the solid–liquid interface. The principle hole traps are commonly believed to be adsorbed hydroxide ions or water molecules (reaction (T2)). Hole trapping (reaction (T6)) proceeds with the formation of hydroxyl radicals. Howe and Grätzel have recently proposed that the fundamental hole trap (at 77 K) is a subsurface lattice oxygen situated directly beneath an adsorbed hydroxide (*53*). At higher temperatures it seems likely that the hole moves to the surface to form the observed OH·:

$$h^+ + Ti^{IV}O^{2-}Ti^{IV}OH^- \rightleftharpoons Ti^{IV}O^-Ti^{IV}OH^- \rightleftharpoons Ti^{IV}O^{2-}Ti^{IV}\rfloor OH\cdot. \quad (1)$$

Formation of the surface OH· requires the abstraction of an electron from the adsorbate, thereby altering if not entirely removing the Ti^{IV}–OH^- bond. Immediately after its formation, the hydroxyl radical is still associated with the Ti^{IV} site because of their proximity. This association is depicted in Table 1 by $Ti^{IV}\rfloor OH\cdot$. At this point we have not specified whether or not the radical is adsorbed. Three possibilities now exist: (i) The hydroxyl radical may interact with the solid by reaction (T6−) or equivalently by the back reaction of Eq. (1); (ii) the radical may attack an adjacent adsorbed or solution-phase molecule (e.g., reaction (T9) or (T11)); or (iii) the radical may diffuse away from its surface formation site and later react with an adsorbed or solution-phase molecule (e.g., reaction (T10) or (T12)). If the hydroxyl radical retains some bond character with Ti^{IV}, perhaps by a rapid resonance with a subsurface oxygen as in Eq. (1), then the radical may be depicted as adsorbed on the semiconductor. Alternately, the radical may be free, yet too reactive to move far from the surface. These two possibilities cannot be distinguished by the analysis of overall kinetics.

By comparing typical reaction and diffusion rates we may determine if the above possibility (iii) is plausible. We define ϕ as the *reaction-diffusion modulus* for OH·, where

$$\phi \equiv \frac{\text{reaction rate}}{\text{diffusion rate}} = \frac{k_{6-}}{D/L^2}. \quad (2)$$

Rothenberger *et al.* (*54*) have determined that the disappearance rate of trapped electrons follows overall first-order kinetics in trapped electron concentration with a first-order rate constant of 5.5×10^5 s^{-1}. The disappearance of trapped electrons results from the recombination of trapped holes and trapped electrons, (i.e., the reaction sequence (T6−), (T8−), (T5)). Since hole trapping is slower than either free carrier recombination (reaction (T5)) or electron trapping (reaction (T8)) (*54*), we can estimate that $k_{6-} = 5.5 \times 10^5$ s^{-1}. Liquid diffusion coefficients, D, are generally $\approx 10^{-9}$ m^2/s (*55*). Finally, if we take the distance at which the OH· no longer "sees" the solid surface as $L = 10^{-9}$ m (10 Å), four to five times the typical Ti–OH^- bond length, we find $\phi \approx 10^{-4}$. This result implies that the average rate of reaction between the photogenerated OH· and the semiconductor surface (reaction (T6−)) is far less than the diffusion rate. Thus, it is plausible for the radical to diffuse away from the surface and to react subsequently in solution (see (*73*), however).

The average distance that a hydroxyl radical can diffuse into solution before reacting may be estimated by a similar expression. The reaction of interest is now that between OH· and any reactant [S] that it may en-

counter (e.g., organics, other radicals, H_2O_2):

$$\phi' = \frac{k_{OH\cdot}[S]}{D/L^2}. \quad (3)$$

Second-order rate constants for OH· are generally on the order of $10^9\ M^{-1}\ s^{-1}$ (*17*). By setting $\phi' = 1$, signifying equal reaction and diffusion rates, we can solve for L and obtain an estimate of the average distance of molecular diffusion before reaction. Note that as reactant concentration $[S]$ increases, this distance diminishes. Using $[S] = 10^{-3}\ M$, we find $L \approx 10^{-8}$ m (100 Å), and for $[S] = 10^{-6}\ M$, $L \approx 10^{-6}$ m. On the basis of these order-of-magnitude calculations, we would not expect OH· to diffuse very far into solution even for very low concentrations of oxidizable reactants. For slurry reactors, where particle-to-particle distances are on the order of microns (*56*), the OH· diffusion length may be large enough to achieve a nearly homogeneous solution of OH·. However, the much greater separation distances involved with immobilized photocatalysts would limit the degradation reaction to a thin fluid film near the photocatalyst surface, thereby raising the possibility of mass transfer controlled kinetics (*56*).

Direct hole–organic reaction (reaction (T7)), while often thermodynamically possible, is not believed to be significant, because of the lack of reactivity witnessed in water-free organic solutions. Recent findings imply that aromatic molecules adsorb to surface hydroxyls rather than directly to the TiO_2 lattice (*57*). For this case, the oxidative attack of the aromatic would be analogous to reaction (T11).

Photo-excited electrons are trapped by Ti^{IV} centers to form Ti^{III} as in reaction (T8-a) (*53*). For systems without a reducible adsorbate, conduction band electrons remain on the semiconductor resulting in the formation of the blue color characteristic of Ti^{III} (*7, 12, 53, 54, 58*). When O_2 is present, the surface Ti^{III} is readily oxidized by molecular oxygen to form the superoxide ion radical (reaction (T8-b) (*26, 48, 53, 59*). Superoxide may be further reduced to H_2O_2 (reaction (T13)) (*47, 48*). Alternatively, under acidic conditions, H^+ may protonate the superoxide to form the perhydroxyl radical (reaction (T14), $pK_a = 4.8$). Interaction between OH·, $HO_2^{\cdot}$, and H_2O_2 is shown as reaction (T15). While these three species have been detected in illuminated aqueous solutions of TiO_2 (*8, 45, 47, 48*), $O_2^{\cdot-}$ has only been unequivocally identified in the gas–TiO_2 system (*60*), and in illuminated solutions of less photo-active semiconductors (*61, 62*).

For the purpose of this study, we assume the dissolved oxygen (DO) concentration remains constant, at least for the early portion of the degradation run. Constant DO concentration throughout the entire run has been obtained experimentally by maintaining a well-mixed oxygen headspace in the reactor (*40*). The dependence of the photocatalytic degradation rate on DO concentration has been modeled successfully by the noncompetitive Langmuir adsorption term (*7, 8*)

$$r \propto \frac{K_{O_2}[O_2]}{1 + K_{O_2}[O_2]}. \quad (4)$$

Noncompetitive adsorption of oxygen agrees with the suggested mechanism, since O_2 is believed to adsorb exclusively on Ti^{III} sites (reaction (T8-b)) while hydroxyls are formed by adsorption at Ti^{IV} and lattice oxygen sites (reaction (T2)).

Reactions (T9) through (T12) represent four different possible pathways for OH· attack on organics, depending on whether the reacting species are on the photocatalyst surface or in the fluid phase. The compound created by the Rideal mechanisms ((T10) and (T11)) may be surface bound or in solution, although it seems likely that reaction (T10) will lead to an adsorbed product and reaction (T11) to a fluid-phase product. If the hole-trapping reaction forms a free hydroxyl radical, the conditions represented by reaction (T4) differ only by the available diffusion time. In this event, there is no

TABLE 3

Derived Kinetic Rate Expressions[a]

$$r_{R_1} = \frac{k_{obs}\kappa_{R1}[R_1]}{1 + \kappa_{R1}[R_1] + \sum_{i=2}^{n}\kappa_{Ri}[R_i]}$$

$$k_{obs} = \alpha a_c k_1 I \qquad \text{(low } I\text{)}$$

$$k_{obs} = \alpha a_s k'_{6+}\left(\frac{k_1 I a_c}{k_5 v_p}\right)^{1/2} \qquad \text{(high } I\text{)}$$

Case	Description	κ_{R_1} (mM^{-1})	κ_{R_i} (mM^{-1})
I	Ti^{IV}|$OH\cdot$, R_{ads}	$\frac{k_9 K_3[site]a_s}{k_{6-}}$	$\frac{k_{R_i}K_{R_i}[site]a_s}{k_{6-}}$
II	$OH\cdot$, R_{ads}	$\frac{k_{10}K_3[site]}{k_{6-}K_4[Ti^{IV}]}$	$\frac{k_{R_i}K_{R_i}[site]}{k_{6-}K_4[Ti^{IV}]}$
III	Ti^{IV}|$OH\cdot$, R	k_{11}/k_{6-}	k_{R_i}/k_6
IV	$OH\cdot$, R	$\frac{k_{12}}{k_{6-}K_4[Ti^{IV}]a_s}$	$\frac{k_{R_i}}{k_{6-}K_4[Ti^{IV}]a_s}$

[a] See Appendix 2.

mechanistic difference between Cases I and II and between Cases III and IV. The rate expressions for Case II are derived in Appendix 2. Largely because reactions (T1)–(T8) remain unchanged for the four cases, all four cases arrive at rate laws of a similar form. The algebraic forms of the kinetic parameters are summarized in Table 3.

Reactions (T13) through (T15) depict routes for the formation of other radical species. These reactions are given for completeness only and are not used here in the formulation of the kinetic rate laws. Numerous other interactions between radical species are possible but are not listed in this paper. For example see Refs. (*8, 37, 45*). The chemical reactions occurring during photocatalysis are clearly numerous and complicated. The challenge to kineticists is to condense the system into a representative rate form of practical use.

DISCUSSION

The expression for r_{R_1} (Table 3) has the appearance of the familiar Langmuir–Hinshelwood kinetic rate law

$$r_i = -\frac{dC_i}{dt} = \frac{k_{obs}\kappa_{obs}C_i}{1 + \kappa_{obs}C_i}. \qquad (5)$$

Equation (5) has been employed to describe the observed photocatalytic initial rate results of single-component systems (*1, 4, 38, 63, 64*). Integrated L–H rate equations, modified to account for possible competitive intermediates, have been shown to fit single-component temporal data (*40*). The assumptions used in the derivation of the equation for r_{R_1} (Table 3) represent the photocatalytic system better than those of the traditional L–H model (see, for example, Ref. (*65*)). One advantage of formulating rate forms from representative assumptions as opposed to empirical observations lies in the ability to predict trend or values for the parameter groups obtained (i.e., k_{obs} and κ_{obs}). An interesting finding of this study is that, irrespective of which of the four cases is considered, the expression for k_{obs} is the same (Table 3). Importantly, k_{obs} is predicted to be a function only of catalyst properties and reaction conditions, and therefore its value should be independent of the particular organic reactant being degraded.

Experimental findings. The usual method for obtaining values for k_{obs} and κ_{obs} (Eq. (5)) is to plot single-component initial rate data as $1/r_i^0$ vs $1/C_i^0$, where r_i^0 is the initial disappearance rate of reactant i, and C_i^0 is the initial concentration of i. Such a plot should be linear if the L–H rate form (Eq. (5)) is representative. The intercept of this line corresponds to $1/k_{obs}$ while the slope is equal to $1/(k_{obs}\kappa_{obs})$. Therefore, if k_{obs} is independent of reactant, as predicted by the derived kinetic rate laws (Table 3), the intercepts should be equal for all reactants degraded in the same reactor and under the same conditions.

Initial rate data are tedious to obtain and prone to variation. When a plot of $1/r^0$ vs $1/C^0$ is constructed, there is often appreciable scatter in the data or few data points. A least-squares line may provide the best fit of the data and result in reasonable

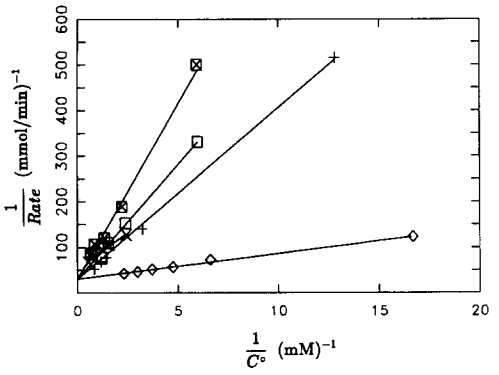

FIG. 2. Reciprocal initial rate vs reciprocal initial concentration for (□) chloroform, (×) dichloromethane, (◇) perchloroethylene (PCE), (⊠) chloroacetic acid, and (+) dichloroacetic acid. Catalyst: 1.0 g/liter Fisher Chemical TiO_2, Lot Nos. 773688 and 745547. Data from Ref. (*66*).

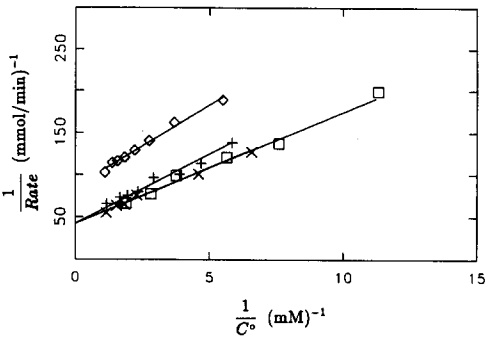

FIG. 4. Reciprocal initial rate vs reciprocal initial concentration for (□) tribromomethane, (×) dibromomethane, (◇) 1,2-dibromoethane, (+) 1,1-dibromoethane. Catalyst: 1.0 g/liter Fisher Chemical TiO_2, Lot No. 773688. Data from Ref. (*68*).

values for k_{obs} and κ_{obs}. Yet, lines that seem equally good can result in substantially different values for the parameters due to the sensitivity of the intercept ($1/k_{obs}$) to adjustments in the line used to fit the data. In contrast, the slope, $1/(k_{obs}\kappa_{obs})$, is fairly insensitive to such adjustments. These observations indicate that we need to consider the original initial rate data rather than the reported L–H parameters when attempting to ascertain if k_{obs} values for different reactants are indeed equal.

Full initial rate data for the photocatalysed degradation of different compounds in the same system are not commonly reported in the literature. Previously reported data from our laboratory for several compounds are shown in Figs. 2–5 [*40*, *66–68*]. With only two exceptions, (1,2-dibromoethane in Fig. 4, and CCl_4, which displayed very limited reactivity and is not plotted), the intercepts appear to be equivalent. The very slow photocatalytic reaction rate of CCl_4 is consistent with the reported negligible rates of reaction between OH· and fully halogenated compounds in homogeneous

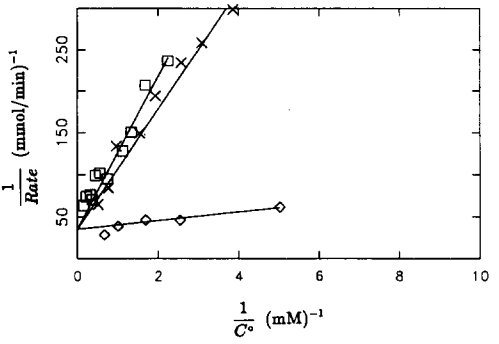

FIG. 3. Reciprocal initial rate vs reciprocal initial concentration for (□) 1,2-dichloroethane, (×) 1,1-dichloroethane, and (◇) vinyl chloride. Catalyst: 1.0 g/liter Fisher Chemical TiO_2, Lot No. 773688. Data from Ref. (*67*).

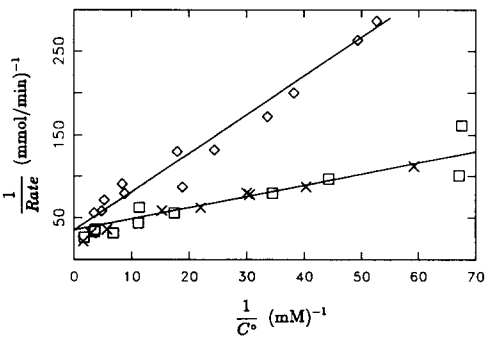

FIG. 5. Reciprocal initial rate vs reciprocal initial concentration for (□, ×) benzene and (◇) perchloroethylene (PCE). Catalyst: 1.0 g/liter Degussa P25 TiO_2, Lot No. RV0167. Data from Ref. (*40*).

systems (*69, 70*). The fact that compounds of different chemical properties like benzene and PCE (Fig. 5) or chloromethanes and carboxylic acids (Fig. 2) achieve the same k_{obs} is compelling. Finally, the absolute values of the intercepts are nearly identical for all four figures, despite the involvement of different investigators. Since all researchers used the same reactor design, lamp configuration, and catalyst loading, this result is in agreement with the model.

The data of Figs. 2–4 employed the same TiO_2 catalyst (Fisher Chemical, Lot 773688). The data of Fig. 5 were obtained with a different photocatalyst (Degussa P25, Lot RV0167). The developed model does not require similar k_{obs} values for different catalyst brands since k_{6+}, k_1, and k_5 should be functions of the semiconductor's physical and electronic properties. Therefore, more data are required to determine if the similarity between the k_{obs} values from Fig. 5 and those of Figs. 2–4 is coincidental or meaningful.

The predicted square-root dependency of reaction rate on intensity has been observed with the illumination intensities typically used (*9, 11*). As discussed in Appendix 2, data obtained at lower illumination levels have shown the transition from first order to square-root dependency with increasing illumination intensity.

From our laboratory results, 14 of 16 different compounds examined have exhibited equal values for k_{obs}, in agreement with our proposed mechanism. The future publication of full initial rate data for different reactants degraded under identical conditions should allow for verification or rejection of this trend.

Prediction of parameters. From Table 3, we predict that κ for Cases III and IV should be proportional to a second-order reaction rate constant for the two reacting species. (Cases I and II predict a κ dependence on the organic's adsorptive properties as well.) If either Case III or IV represents the true mechanism, it should be possible to correlate the κ parameters with

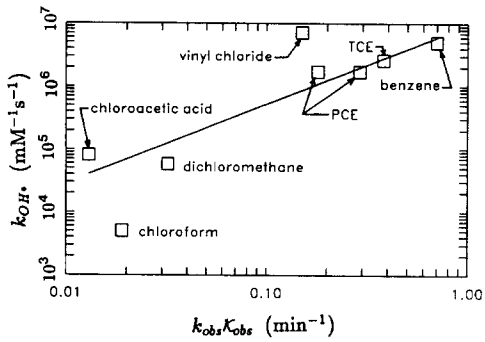

FIG. 6. Comparison of the product of observed photocatalytic degradation rate constants with tabulated second-order rate constants for reaction with OH· (*17, 72*). The kinetic model, Table 3, predicts a direct proportionality between $k_{OH\cdot}$ and $k_{obs}\kappa_{obs}$.

second-order rate constants for the solution-phase reaction of OH· and organics. Many of these homogeneous rate constants, which we will denote as $k_{OH\cdot}$, have been measured (*17*). For Case III we must assume that the rate constant for a surface-associated OH· is proportional to its homogeneous solution value. Note that, according to the derived model, $k_{OH\cdot} = k_{12}$. We will compare tabulated $k_{OH\cdot}$ values with $k_{obs}\kappa_{obs}$, since this product, while still predicted to be proportional to $k_{OH\cdot}$, is less sensitive to experimental interpretation. Figure 6 displays results for compounds for which both reliable kinetic rate data and aqueous hydroxyl radical reaction rate constants are available. The degradation data in this figure were taken with the same reactor configuration but sometimes involved different catalyst brands.

If a proportionality exists between $k_{OH\cdot}$ and $k_{obs}\kappa_{obs}$, we would expect the data of Fig. 6 to fall on a straight line with a slope of unity on a log-log plot. The results are suggestive but not conclusive. While six of the eight data points correlate reasonably well, those of vinyl chloride and chloroform do not follow the same pattern. (Two points are available for PCE because this compound has been studied by two different researchers.) Because of the effects of pH and other experimental variables, more

data are required to establish a clear trend. Also, if the actual mechanism resembles Cases I or II, the affinity for adsorption of each organic will affect κ, and a direct proportionality to $\kappa_{OH\cdot}$ would not result. In any event, Fig. 6 shows that a correlation between $k_{OH\cdot}$ and $k_{obs}\kappa_{obs}$ is plausible.

Previous researchers have attempted to equate photocatalytic degradation rates with tabulated $k_{OH\cdot}$ values (*71*). No correlation was found, partly because of the difficulty in finding appropriate literature hydroxyl rate constants for the compounds examined in that study. Additionally, the comparison is usually made between the "kinetic rate constant," k_{obs} (or a pseudo-first-order rate constant), and $k_{OH\cdot}$. Our model predicts that k_{obs} is unrelated to hydroxyl rate constants and that pseudo-first-order rate constants will often be functions of reactant concentration (for large κ_R or $[R]$). Rather, it is κ_{obs} which is predicted to be a function of radical second-order rate constants (Table 3).

Rothenberger *et al.* (*54*) have used laser pulse photolysis coupled with nano- and picosecond spectroscopy to estimate carrier trapping and recombination rates in an aqueous semiconductor slurry. These phenomena correspond to reactions (T5), (T6), and (T8) in Table 1. Therefore, one should be able to obtain estimates for k_5, k_{6+}, and k_{8+} for a given photocatalyst by pulse photolysis. By analyzing the rate of recombination between trapped electrons and trapped holes, the rate-determining step in the back reaction (reaction sequence (T6−), (T8−), and (T5)) may be determined. This step is believed to be reaction (T6−). With the additional knowledge of the absorbed photon flux ($k_1 I a_c$) and catalyst physical properties (a_s, v_p, etc.), one may be able to estimate both k_{obs} and κ_{obs}.

As an example, we can estimate κ for the simplest case (Case III) if we assume $k_{11} = k_{OH\cdot}$. From the results of Rothenberger *et al.*, we estimate that $k_{6-} = 5.5 \times 10^5\ s^{-1}$. The comparison of κ_{est} vs the experimental values κ_{obs} determined from Figs. 2–5 is shown in Table 4. There are numerous reasons for the estimated κ values to vary from the observed degradation results; e.g., Case III may not have been the true mechanism, different catalyst brands were used, and there were variations in the conditions under which $k_{OH\cdot}$ was determined. Therefore, the comparison in Table 4 is meant as an example of how κ values may be predicted and is not intended to prove or disprove the validity of Case III. Considering these stipulations, agreement of a number of (κ_{obs}, κ_{est}) pairs within a factor of 3 (last column, Table 4) is quite good.

TABLE 4

Estimation of κ Constants for Case III

Compound	κ_{obs} (mM^{-1})	κ_{est} (mM^{-1})	$\kappa_{obs}/\kappa_{est}$
Chloroform	5.7×10^2	9.1×10^0	63
Dichloromethane	9.7×10^2	1.0×10^2	9.7
Chloroacetic acid	3.9×10^2	1.5×10^2	2.6
Perchloroethylene (PCE)	5.4×10^3	3.1×10^3	1.7
	1.0×10^4		3.2
Trichloroethylene (TCE)	1.5×10^2	4.7×10^3	0.032
Benzene	2.4×10^4	9.1×10^3	2.6
Vinyl chloride	5.2×10^3	1.3×10^4	0.40

Note. Experimentally observed value for TCE from (*64*), others from Figs. 2–5.

CONCLUSIONS/SUGGESTED WORK

This work has demonstrated that many possible mechanisms can give rise to the Langmuir–Hinshelwood rate forms commonly used to describe photocatalytic degradation kinetics. The cases in this study were all based on the assumption that the hydroxyl radical is the primary oxidant in the photocatalytic system. We have shown that the prediction of a reactant-independent rate parameter, k_{obs}, is verified by the results of our laboratory. Further evidence may be obtained if other research groups publish their complete initial rate data. Additionally, a correlation between second-order hydroxyl radical reaction rate constants and observed degradation constants (κ) seems likely.

At this point, it is not possible to distinguish between the reaction of an adsorbed radical and the reaction of a free radical very near to the photocatalyst surface. However, from comparisons of reaction and diffusion rates, we find it plausible that OH· is present as a mobile radical. Because of its high reactivity, the radical is unable to diffuse very far from the surface before reacting. For surface-generated free radicals, adsorption of the organic substrate would be an aid but not a requirement for reaction. Under these assumptions, the oxidative degradation reaction could be a combination of Cases II and IV, where photo-generation of free OH· is given by the sum of reactions (T6+) and (T4−). Since the root-mean-square diffusion distance is inversely proportional to the concentration of oxidizable reactants, perhaps the analysis of ultrapure aqueous systems (involving an immobilized photocatalyst) or vapor–solid photocatalytic systems will allow for the detection of free hydroxyl radicals.

The fate of oxygen has not been explored in the development of these mechanisms. Further investigation of oxygen reduction, via isotope studies and other techniques, may lead to additional insights into the true degradation mechanism(s). In addition, the use of laser pulse photolysis to investigate the rapid recombination and trapping events occurring in and on the semiconductor photocatalyst may allow for the measurement of the kinetic parameters derived for the proposed mechanisms.

Although it is not yet possible to distinguish which (if any) of the proposed cases represent the actual degradation mechanism, this study has demonstrated the utility of plausible kinetic mechanisms for the description of observed phenomena and the prediction of model parameters. As has historically occurred in the study of chemical reaction kinetics, the development of representative reaction mechanisms will undoubtedly advance efforts to predict and modify photocatalytic reaction kinetics.

APPENDIX 1: NOMENCLATURE

Arabic:

- a_c = Photocatalyst particle area normal to illumination, m^2.
- a_s = Particle surface area, m^2.
- D = Molecular diffusivity, m^2/s.
- h^+ = Semiconductor valence band hole.
- I = Illumination intensity, einstein m^{-2} s^{-1}.
- k = Reaction rate constant.
- K = Equilibrium adsorption constant, m^3 mol^{-1}.
- L = Characteristic diffusion length, m.
- r = Degradation rate, mol s^{-1} particle^{-1}.
- v_p = Particle volume, m^3.

Greek

- α = Proportionality constant.
- κ = Kinetic parameter, hydroxyl radical reaction ratio, m^3 mol^{-1}.

Subscripts

Arabic numbers refer to reactions in Table 1.

- +,− Refer to the forward or back reaction, respectively.
- obs = Observed value from degradation experiments.
- est = Value estimated based on model assumptions.

APPENDIX 2

We begin by considering a single catalyst particle under uniform illumination in an aqueous solution. A summary of the possible reactions occurring during the photocatalytic degradation reaction is given in Table 1. Each of the four cases presented in Table 3 uses selected reactions from this set. We present the derivation of Case II to illustrate the assumptions of the kinetic model.

Case II represents the most complex mechanism since the surface-generated OH· must diffuse into solution and the organic reactant, which normally originates in the solution phase, must adsorb. In this scheme, the reactions of interest are (T1)–

(T6), (T8), and (T10). As discussed in the text, reaction (T7) is assumed to be insignificant. For the single photocatalyst particle, the rate of disappearance of the reactant of interest, R_1, may be represented by

$$r_{II} = k_{10}[\text{OH}\cdot][R_{1,\text{ads}}]a_s. \quad (6)$$

We now invoke the steady-state approximation for the *total* concentration of OH· present:

$$\frac{d[\text{OH}\cdot]_t}{dt} = \alpha k_{6+}[h^+][\text{Ti}^{\text{IV}}(\text{OH})]a_s - k_{6-}[\text{Ti}^{\text{IV}}\text{OH}\cdot]a_s - k_{10}[\text{OH}\cdot][R_{1,\text{ads}}]a_s - \sum_{i=2}^{n} k_{R_i}[\text{OH}\cdot][R_{i,\text{ads}}]a_s \approx 0. \quad (7)$$

In this expression, n represents the number of different organic species present and $[\text{Ti}^{\text{IV}}(\text{OH})]$ represents the surface concentration of bound OH^- or H_2O which can react with valence band holes, h^+. This latter concentration should remain relatively constant in an aqueous system; that is, the equilibrium of reaction (T2) lies far to the right. Thus, we may define $k'_{6+} = k_{6+}[\text{Ti}^{\text{IV}}(\text{OH})]$.

The constant α is necessary to account for possible radical formation via the reduction of O_2 by conduction band electrons (see Eqs. (T13)–(T15)) (*8*). The constraint of electroneutrality on a catalyst particle maintains that one e^- must react per h^+ reacted. If reduction of O_2 leads to net radical formation, there will be an increase in the number of photo-generated radicals proportional to their production rate by reaction (T6). The α term is the proportionality constant. We expect $1 \leq \alpha \leq 2$, since stoichiometry and redox considerations indicate that the trapping of one conduction band electron can result in a maximum net gain of only one radical.

There are two methods by which the surface-generated OH· can appear in the bulk solution. If hole trapping produces a free hydroxyl radical, this species has only to diffuse away from the surface. If, however, the hydroxyl radical retains some residual bond character to titanium (see text, Eq. (1)), it must first desorb. This condition is governed by reaction (T4). These two possibilities are described by either the two-step process of reactions (T6+) and (T4−) in sequence or by a single step consisting of the sum of reactions (T6+) and (T4−). The only difference in these two possibilities will be the presence or absence of the equilibrium adsorption constant, K_4 (where $K_4 \equiv k_{4+}/k_{4-}$), in the derived rate expression. For the purpose of this derivation, we will use the more general case involving the adsorption constant; thus $[\text{Ti}^{\text{IV}}\text{OH}\cdot] = K_4[\text{OH}\cdot][\text{Ti}^{\text{IV}}]$. Thus we have

$$\alpha k'_{6+}[h^+] - k_{6-}K_4[\text{OH}\cdot][\text{Ti}^{\text{IV}}] - k_{10}[\text{OH}\cdot][R_{1,\text{ads}}] - \sum_{i=2}^{n} k_{R_i}[\text{OH}\cdot][R_{i,\text{ads}}] = 0$$

or

$$[\text{OH}\cdot] = \frac{\alpha k'_{6+}[h^+]}{k_{6-}K_4[\text{Ti}^{\text{IV}}] + k_{10}[R_{1,\text{ads}}] + \sum_{i=2}^{n} k_{R_i}[R_{i,\text{ads}}]}. \quad (8)$$

Similarly, if we use the steady-state approximation for the concentration of holes, we obtain

$$\frac{d[h^+]}{dt} = k_1 I a_c - k'_{6+}[h^+]a_s + k_{6-}[\text{Ti}^{\text{IV}}\text{OH}\cdot]a_s - k_5[h^+][e^-]v_p \approx 0. \quad (9)$$

Because of the photo-generation rates of h^+ and e^- are equal, and because the semiconductor intrinsic carrier density is comparatively low (*11*), we may assume $[h^+] = [e^-]$:

$$k_1 I a_c = k'_{6+}[h^+]a_s - k_{6-}[\text{Ti}^{\text{IV}}\text{OH}\cdot]a_s + k_5 v_p[h^+]^2. \quad (10)$$

Recent laser pulse photolysis studies have shown that the rate constants for free car-

rier recombination (k_5) and electron trapping are much greater than those for hole trapping (k_{6+}, k_{6-}) (*54*). Therefore, when $[h^+]$ is high, we expect

$$k_5 v_p [h^+]^2 \gg k'_{6+}[h^+]a_s - k_{6-}[\mathrm{Ti^{IV}OH\cdot}]a_s.$$

Under these conditions, Eq. (10) simplifies to

$$[h^+]_{high} = \left(\frac{k_1 I a_c}{k_5 v_p}\right)^{1/2}. \quad (11)$$

Although $k_5 \gg k'_{6+}$, the hole-trapping reaction is able to compete effectively with recombination at very low hole concentration because of the $[h^+]^2$ dependence of recombination. For very low electron-hole generation rates, Rothenberger *et al.* (*54*) have shown that the disappearance of trapped electrons follows overall first-order kinetics. It is postulated that this is due to reaction (T6−) being the rate-determining step in the reaction between trapped holes and trapped electrons (the reaction sequence (T6−), (T8−), (T5)). Therefore, for low $[h^+]$, Eq. (10) will simplify to

$$[h^+]_{low} = \left(\frac{k_1 I a_c + k_{6-}[\mathrm{Ti^{IV}OH\cdot}]a_s}{k'_{6+}a_s}\right). \quad (12)$$

Since high carrier densities are created by high photon fluxes, the regimes of Eqs. (11) and (12) correspond to high and low illumination intensities, respectively. Experimental observations show that the dependence of the photocatalytic degradation rate on illumination intensity undergoes a transition from first-order to half-order kinetics as intensity increases (*9, 11*). The first-order dependence is obtained if $k_1 I a_c \gg k_{6-}[\mathrm{Ti^{IV}OH\cdot}]a_s$ in Eq. (12). Since reaction (T6−) is merely one path for the deexcitation of the photo-generated OH·, it is clear that at least $k_1 I a_c \geq k_{6-}[\mathrm{Ti^{IV}OH\cdot}]a_s$.

For most photochemical applications, appreciable intensities are desired. Therefore, we will deal with the situation where Eq. (11) describes the illumination dependence. Substitution of Eq. (11) into Eq. (8) gives

$$[\mathrm{OH\cdot}] = \frac{\alpha k'_{6+}\left(\frac{k_1 I a_c}{k_5 v_p}\right)^{1/2}}{k_{6-}K_4[\mathrm{Ti^{IV}}] + k_{10}[R_{1,ads}] + \sum_{i=2}^{n} k_{R_i}[R_{i,ads}]}. \quad (13)$$

Finally, combining Eqs. (6) and (13), and employing reaction (T3) to describe the adsorption of organic species, $[R_{1,ads}] = K_3[R_1][\mathrm{site}]$, we obtain

$$r_{II} = \frac{k_{obs}\kappa_{R_1}[R_1]}{1 + \kappa_{R_1}[R_1] + \sum_{i=2}^{n} \kappa_{R_i}[R_i]}, \quad (14)$$

where

$$k_{obs} = \alpha a_s k'_{6+}\left(\frac{k_1 I a_c}{k_5 v_p}\right)^{1/2}$$

$$\kappa_{R_1} = \frac{k_{10}K_3[\mathrm{site}]}{k_{6-}K_4[\mathrm{Ti^{IV}}]}$$

$$\kappa_{R_i} = \frac{k_{R_i}K_{R_i}[\mathrm{site}]}{k_{6-}K_4[\mathrm{Ti^{IV}}]}.$$

For organic compounds which adsorb on $\mathrm{Ti^{IV}}$ sites, the ratio $[\mathrm{site}]/[\mathrm{Ti^{IV}}]$ in the expressions for κ_{R_1} and κ_{R_i} will become unity. Table 3 lists the kinetic parameter forms obtained for all four cases.

ACKNOWLEDGMENTS

The authors thank Sandia National Laboratories for partial support during the formulation of this paper. C. S. Turchi also thanks the National Science Foundation and Du Pont for financial support. Finally, we appreciate the assistance of Professors H. Henry Lamb and P. K. Lim for their knowledge of surface and radical chemistry and Ed Wolfrum for numerous topical discussions.

Note added in proof. New ESR evidence implies reaction of ·OH at the photocatalyst surface (personal communication, J. Bolton, Chemistry Dept., Univ. of Western Ontario, Canada).

REFERENCES

1. Ollis, D. F., *Environ. Sci. Technol.* **19,** 480 (1985).
2. Barbeni, M., Pramauro, E., Pelizzetti, E., Borgarello, E., Serpone, N., and Jamieson, M. A., *Chemosphere* **15,** 1913 (1986).

3. Hidaka, H., Kubota, H., Grätzel, M., Pelizzetti, E., and Serpone, N., *Nouv. J. Chim.* **9,** 67 (1985).
4. Matthews, R., *Water Res.* **20,** 569 (1986).
5. Matthews, R., *Aust. J. Chem.* **40,** 667 (1987).
6. Pelizzetti, E., Barbeni, M., Pramauro, E., Serpone, N., Borgarello, E., Jamieson, M., and Hidaka, H., *Chim. Ind. (Milan)* **67,** 623 (1985).
7. Sczechowski, J., M.S. thesis, North Carolina State Univ., 1988.
8. Okamoto, K., Yamamoto, Y., Tanaka, H., Tanaka, M., and Itaya, A., *Bull. Chem. Soc. Japan* **58,** 2015 (1985).
9. Okamoto, K., Yamamoto, Y., Tanaka, H., and Itaya, A., *Bull. Chem. Soc. Japan* **58,** 2023 (1985).
10. Tunesi, S., and Anderson, M. A., *Chemosphere* **16,** 1447 (1987).
11. Egerton, T. A., and King, C. J., *J. Oil Col. Chem. Assoc.* **62,** 386 (1979).
12. Bahnemann, D., Henglein, A., Lilie, J., and Spanhel, L., *J. Phys. Chem.* **88,** 709 (1984).
13. Heller, A., Degani, Y., Johnson, D. W., and Gallagher, P. K., *J. Phys. Chem.* **91,** 5987 (1987).
14. Al-Ekabi, H., and Serpone, N., *J. Phys. Chem.* **92,** 5726 (1988).
15. Serpone, N., Borgarello, E., Harris, R., Cahill, P., Borgarello, M., and Pelizzetti, E., *Solar Energy Mater.* **14,** 121 (1986).
16. Matthews, R., *J. Phys. Chem.* **91,** 3328 (1987).
17. Farhataziz, and Ross, A. B., "Selected Specific Rates of Reactions of Transients from Water in Aqueous Solution. III. Hydroxyl Radical and Perhydroxyl Radical and their Radical Ions," NSRDS-NBS 59, National Bureau of Standards, 1977.
18. Augustynski, J., "Structure and Bonding," vol. 69, Springer-Verlag, Berlin, 1988.
19. Parfitt, G. D., *Prog. Surf. Membr. Sci.* **11,** 181 (1976).
20. Boehm, H. P., and Herrmann, M., *Z. Anorg. Chem.* **352,** 156 (1967).
21. Boehm, H. P., *Discuss. Faraday Soc.* **52,** 264 (1971).
22. Suda, Y., and Morimoto, T., *Langmuir,* **3,** 786 (1987).
23. Tanaka, K., and White, J. M., *J. Phys. Chem.* **86,** 4708 (1982).
24. Morishige, K., Kanno, F., Ogawara, S., and Sasaki, S., *J. Phys. Chem.* **89,** 4404 (1985).
25. Boonstra, A. H., and Mutsaers, C. A. H. A., *J. Phys. Chem.* **79,** 1694 (1975).
26. Munuera, G., Rives-Arnau, V., and Saucedo, A., *J. Chem. Soc. Faraday Trans. 1* **75,** 736 (1979).
27. Doremieux-Morin, C., Enriquez, M. A., Sanz, J., and Fraissard, J., *J. Colloid Interface Sci.* **95,** 502 (1983).
28. Fujihira, M., Satoh, Y., and Osa, T., *Bull. Chem. Soc. Japan* **55,** 666 (1982).
29. Fujishima, A., Inoue, T., and Honda, *K., J. Amer. Chem. Soc.* **101,** 5582 (1979).
30. Grätzel, M., *Ann. Chim. (Rome)* **77,** 411 (1987).
31. Bard, A., Ed., *"Encyclopedia of Electrochemistry of the Elements,"* Vol. 2, p. 192. Dekker, New York, 1974.
32. Fox, M.-A., and Chen, C., *J. Amer. Chem. Soc.* **103,** 6757 (1981).
33. Fujihira, M., Satoh, Y., and Osa, T., *J. Electroanal. Chem.* **126,** 277 (1981).
34. Barbeni, M., Pramauro, E., Pelizzetti, E., Borgarello, E., Gratzel, M., and Serpone, N., *Nouv. J. Chim.* **8,** 547 (1984).
35. Cunningham, J., and Srijaranai, S., *J. Photochem. Photobio. A: Chem.* **43,** 329 (1988).
36. Augugliaro, V., Palmisano, L., Sclafani, A., Minero, C., and Pelizzetti, E., *Toxicol. Environ. Chem.* **16,** 89 (1988).
37. Al-Ekabi, H., Serpone, N., Pelizzetti, E., Minero, C., Fox, M. A., and Draper, R. B., *Langmuir* **5,** 250 (1989).
38. Ollis, D. F., Hsiao, C., Budiman, L., and Lee, C., *J. Catal.* **88,** 89 (1984).
39. Barbeni, M., Morello, M., Pramauro, E., Pelizzetti, E., Vincenti, M., Borgarello, E., and Serpone, N., *Chemosphere* **16,** 1165 (1987).
40. Turchi, C. S., and Ollis, D. F., *J. Catal.* **119,** 480 (1989).
41. Metelitsa, D. I., *Russ. Chem. Rev. Engl. Trans.* **119,** 480 (1989). **40,** 7 (1971).
42. Cox, R. A., Derwent, R. G., and Williams, M. R., *Environ. Sci. Technol.* **14,** 57 (1980).
43. Barbeni, M., Minero, C., Pelizzetti, E., Borgarello, E., and Serpone N., *Chemosphere* **16,** 2225 (1987).
44. Ceresa, E. M., Burlamacchi, L., and Visca, M., *J. Mater. Sci.* **18,** 289 (1983).
45. Jaeger, C. D., and Bard, A., *J. Phys. Chem.* **83,** 3146 (1979).
46. Gonzalez-Elipe, A. R., Munuera, G., and Soria, J., *J. Chem. Soc. Faraday Trans. 1* **75,** 748 (1979).
47. Clechet, P., Martelet, C., Martin, J. R., and Olier, R., *Electrochim. Acta* **24,** 457 (1979).
48. Harbour, J. R., and Hair, M. L., *J. Phys. Chem.* **83,** 652 (1979).
49. Anpo, M., Shima, T., and Kubokawa, Y., *Chem. Lett.,* 1799 (1985).
50. Matthews, R., *J. Chem. Soc. Faraday Trans. 1* **80,** 457 (1984).
51. Völz, H. G. Kämpf, G., and Klaeren, A., *Farbe + Lack* **82,** 805 (1976).
52. Völz, H. G., Kämpf, G., Fitzky, H. G., and Klaeren, A., *ACS Sym. Ser.* **151,** 163 (1981).
53. Howe, R. F., and Grätzel, M., *J. Phys. Chem.* **89,** 4495 (1985).
54. Rothenberger, G., Moser, J., Grätzel, M., Serpone, N., and Sharma, D. K., *J. Amer. Chem. Soc.* **107,** 8054 (1985).
55. Reid, R. C., Prausnitz, J. M. and Sherwood, T. K., "The Properties of Gases and Liquids," 3rd ed., p. 576. McGraw–Hill, New York, 1977.

56. Turchi, C. S., and D. F. Ollis, *J. Phys. Chem.* **92,** 6852 (1988).
57. Nagao, M., and Suda, Y., *Langmuir* **3,** 786 (1987).
58. Kölle, U., Moser, J., and Grätzel, M., *Inorg. Chem.* **24,** 2253 (1985).
59. Munuera, G., Gonzalez-Elipe, A. R., Rives-Arnau, V., Navio, A., Malet, P., Soria, J., Conesa, J. C., and Sanz, J., *in* "Adsorption and Catalysis on Oxide Surfaces" (M. Che and G. C. Bond, Eds.). Elsevier, Amsterdam, 1985.
60. Howe, R. F., and Grätzel, M., *J. Phys. Chem.* **91,** 3906 (1987).
61. Anpo, M., Aikawa, N., and Kubokawa, Y., *J. Chem. Soc. Chem. Commun.*, 644 (1984).
62. Harbour, J. R., and Hair, M. L., *J. Phys. Chem.* **81,** 1791 (1977).
63. Matthews, R., *J. Catal.* **111,** 264 (1988).
64. Pruden, L., and Ollis, D., *J. Catal.* **82,** 404 (1983).
65. Hill, C. G., "Chemical Engineering Kinetics and Reactor Design. "Wiley, New York, 1977.
66. Hsiao, C., M. S. thesis, Univ. of California at Davis, 1983.
67. Gauron, M. R., M. S. thesis, Univ. of California at Davis, 1983.
68. Nguyen, T. C., M. S. thesis, Univ. of California at Davis, 1983.
69. Watson, R. T., Machado, G., Conaway, B., Wagner, S., and Davis, D. D., *J. Phys. Chem.* **81,** 256 (1977).
70. Bjarnov, E., Munk, J., Nielsen, O. J., Pagsberg, P., and Sillesen, A., "Kinetics of the Reaction of Hydroxyl Radicals with Ethane and a Series of Chlorine- and Fluorine-Substituted Methanes at 300–400 K," RISO-M-2366 Report. Risoe Natl. Lab., Roskilde, Denmark, 1982.
71. DeBerry, D. W., Viehbeck, A., Peyton, G. R., and Karpinski, M., "Investigation of Photocatalytic Oxidation for Wastewater Cleanup and Reuse," No. RU-83/12. US Dept. of Interior, 1983.
72. Emmi, S. S., Beggiato, G., Casalbore-Miceli, G., and Fuochi, P. G., *J. Radioanal. Nucl. Chem. Lett.* **93,** 189 (1985).